

# Experimental Analysis of Aerodynamic Characteristics of NACA 0012 Wing Model with Multiple Winglets

*Md. Zadid Iqbal, Abdullah Al-Faruk\*, Md. Ashraf Islam*

Department of Mechanical Engineering, Khulna University of Engineering & Technology, Khulna-9203, Bangladesh

Received: March 16, 2025, Revised: March 25, 2025, Accepted: March 27, 2025, Available Online: March 30, 2025

## ABSTRACT

Downwash in the wing causes a reduction of lift and generates an additional drag, known as the lift-induced drag or the vortex drag for the finite wing. This induced drag ultimately deteriorates the aerodynamic performance of the aircraft. The technical potentiality of multi-winglets is examined in this work to reduce the induced drag without enlarging the wing's span. Aerodynamic characteristics of the NACA 0012 airfoil section-built wing model with gradual increase of winglets have been studied using a subsonic wind tunnel of 1 m × 1 m × 1 m rectangular test section. An untwisted wing model tapered toward tip was constructed using the NACA 0012 airfoil sections for the wind tunnel experiments. Airfoil-shaped wooden plates of the same airfoil profile were used to make the winglets. Experiments were carried out on the wing with the winglets at 0°, 5°, 10° and 15° incidence angles. The results show that the wing with a gradual increase from one winglet to three winglets can reduce the induced drag and improve the aerodynamic performance. The lift coefficient increases up to 21.2%, and the drag coefficient decreases up to 27.2% when multiple winglets are attached with wing mode compared to single winglet. Enhancing lift performance, reducing vortex drag, and improving overall aerodynamic efficiency in multi-winglet configuration can improve fuel efficiency, leading to better aircraft performance.

Keywords: NACA 0012 Wing, Winglets, Lift-induced Drag, Aerodynamic Characteristics, Wind Tunnel Experiment.



Copyright © All authors

This work is licensed under a [Creative Commons Attribution-Non Commercial 4.0 International License](https://creativecommons.org/licenses/by-nc/4.0/).

## 1 Introduction

The most significant lift providing component of an aircraft is the wing. The wing has a streamlined- cross-sectional shape called an airfoil. When the wing moves through the air, the airfoil creates the lift due to the pressure distribution around the airfoil. The average pressure is higher at the airfoil's lower surfaces than that of the upper surface. This pressure difference is the reason for an aerodynamic force whose parallel and perpendicular components for the airfoil chord are defined as lift and drag [1]. When an aircraft moves forward with a velocity, a secondary circulatory motion of air is created around the wingtip because of the pressure difference between the upper and lower surfaces of the wing. This circulatory motion called the wingtip vortices, tends to leak the air from the lower to the upper wing surface, creating a downward velocity component called the downwash [2]. In a typical aircraft design, the wings are attached at their free ends to the fuselage. The outer tips are typically at a higher position than the root tips which make an upward angle with the horizontal plane known as the dihedral. Dihedral is vital for aircraft stability that helps to keep the airplane from rolling accidentally during flight [3]. Wings also carry the fuel for the power plant of the airplane. The mass of the fuel significantly affects instantaneous weight and the airplane's center of gravity.

The designers have created a variety of wings with different aerodynamic properties, mainly based on the subjective purpose and type of the aircraft. For the dispersion of pulverized fluid, the wingtip vortex had been found as an essential factor, and hence the application of agricultural airplanes was introduced. Comparison of several wingtip devices and analysis of the effects on pulverization had been reflected in the work of Coimbra and Catalano [4]. Wingtip devices are usually intended to enhance the aerodynamic efficiency of fixed-wing aircraft. Several types of wingtip devices have been proposed for managing the wake

created by the tip vortices in different manners [5]. The wingtip devices can also improve the aircraft's stability characteristics. The wingtip devices are also valued for their aesthetic appeal of the aircraft from a marketing standpoint.

In general aviation, wingtip devices were significant concerns for gliders, which have been researched in primitive ways even though the wings possess a large aspect ratio. Smith et al. [6] mentioned the development work of winglets for sailplanes experimenting on scale models using wind tunnels. It was demonstrated that adding a single winglet onto the biplanes increased the lift-curve slope and the maximum lift coefficient and calculated a 13% improvement in the vehicle's endurance. Kroo et al. [7] dealt with winglets in a wider concept of non-planar wings. In that study, different types of wings, like box wings, nag wings, etc., were reviewed along with non-planar wakes wings exploited in general. A key constraint in design interest for many aircraft is the potentiality for lowering the vortex drag without increasing the span. Yates and Donald [8] concluded that for small transporter airplanes, single winglets are advantageous; they provide 10% lower induced drag compared to the plain wing of elliptical shape. Ismail et al. [9] conducted an experimental study to measure the effect of the angle of attack on the NACA 4415 wing and found that the wing is more efficient at a lower speed than a higher speed. Al-Atabi [10] investigated devices akin to the wing tip airfoils, named "wing tip sails", on the wingtip fuel tank of a trainer aircraft for fuel use. After the wind tunnel testing of such sails up to four, the reduction of fuel consumption between 3.5% and 5% was demonstrated and confirmed by the flight test experiments. An experimental and numerical investigation by Eftekhari and Al-Obaidi [11] on the finite wing at low Reynold's number established that the drag force acting on the airfoil increases with the increase of incidence angle due to the change of laminar to

\*Corresponding Author Email Address: [alfaruk@me.kuet.ac.bd](mailto:alfaruk@me.kuet.ac.bd)

turbulent flow. Cerón-Muñoz and Catalano [12] experimented on the adaptive multi-winglets through variation of winglet cant angle and showed a decrease in wake turbulence from the winglets in the wing. They concluded that the symmetrically designed winglets were the best for general aviation aircraft and less effective on the tapered wings.

Aerodynamic characteristics for the wing model of the NACA 4315 section without and with winglets of rectangular, triangular, and circular type had been investigated experimentally in a subsonic wind tunnel by Inam et al. [13]. They suggested that the triangular winglet at 5° inclination has the best performance providing a 30.9% reduction in drag compared to other configurations for the maximum Reynolds number considered. The effect of the cant angle of blended type winglet are numerically studied on the aerodynamic characteristics and compared the performance with the plane wing without winglet of the same wing model [14], [15]. It has been concluded that 90° cant-angled winglets exhibit the best performance in terms of lift coefficient, drag coefficient, lift-to-drag ratio, and stall angle of attack compared to other cant-angled winglet models and the plain wing without winglet. Yusoff et al. [16] investigated the evolution of induced drag in Unmanned Aerial Vehicles (UAVs) for a fixed Reynolds number utilizing up to seven winglets arranging them in different cant angle on NACA 23015 profile. The study demonstrated better aerodynamic characteristics at low angle of attack through the reduction of induced drag. Reddy et al. [17] numerically studied a multi-objective optimization of aerodynamic shape for wing-tail-body aircraft configuration consisting of 33 parameters using modelFRONTIER for four simultaneous objectives. The study concluded that Pareto-optimized multi-element winglet demonstrated better performance at high-speed flight regime of subsonic and transonic speeds. Padmanathan et al. [18] conducted a parametric optimization study on novel winglet designs such as, multi-tip, bird-type, twisted etc. for transonic aircraft. The numerical study compared the optimized winglet design with the baseline model (NASA common research model) and reported 18.29% improvement in aerodynamic efficiency by Taguchi method and that of 20.77% by T-GRA coupled with the PCA method. Bio-inspired wing tip devices are numerically investigated by Sethunathan et al. [19] aiming to reduce the wing-tip vortices at low and medium-range Reynolds numbers. The study incorporates three- and four-tipped multiple winglets by making different combinations through varying the cant angle of each tip and reported 22-23% increase in aerodynamic efficiency and better stability compared to straight wing. Bala et al. [20] computationally examined the flow field over a transonic wing which incorporates four different winglet model based on the cant angle and analyzed the pressure variation along with coefficients relevant of wing model.

Moreover, a wing with multiple winglets has the potential to give some other benefits. Having two or multiple winglets in the wing reduces the climb thrust. A winglet-equipped aircraft can typically take a 3% increase in the lift coefficient over the non-winglet equivalent aircraft. This can extend engine life and reduce maintenance costs [21]. If no or single winglets form a wing, it increases cruise thrust. Cruise fuel flow is reduced by up to 6%, saving fuel costs and increasing range. It also improves cruise performance. Winglets can allow aircraft to reach higher levels sooner [22]. Ulrich et al. [23] employed WINGGRID devices experimentally for the reduction of induced drag. The study concluded that multiple winglets can reduce induced drag by approximately 20% using multiple winglets. As wings with

multiple winglets improve fuel efficiency, the noise effects can be significantly reduced due to vortex effects [24]. Consequently, it also reduces carbon emissions. It surely can be advantageous and helpful in air traffic control as it reduces cyclone-type effect/turbulence [25]. However, the appearance has been better than the typical winglet design. Winglets bring a modern look and feel to aircraft and improve customers' perceptions of the airline.

Appraising the literature mentioned above, it is demonstrated that aircraft of any type with winglets attached to the wing have aerodynamically better performance than those without winglets. Previous studies examined multiple winglets of different types at different orientation on the diverge arrangements with fixed or moveable wings which are mostly conducted through numerical approach. However, there are lack of experimental investigations. Moreover, no studied are found that take the NACA 0012 profile for both the wing and winglet in experimental research. In this experimental work, NACA 0012 wing model has been investigated that is attached in a near perpendicular plane with a streamlined, airfoil-shaped plate at the outer tip as winglet and then gradually increased the number of winglets up to three. The winglets were placed side by side at the tip, and additional winglets were slightly canted outward from the fuselage. Aerodynamic characteristics for the wing model with a gradual increase of winglets have been compared and presented. Reynolds number dependence on the aerodynamic performance is examined for varying the angle of attack in this work.

## 2 Wing Model Description and Construction

This study uses a symmetric NACA 0012 airfoil section to make the finite wing. The equation of thickness distribution for a symmetrical 4-digit NACA airfoil is given by

$$y_t = 5t \left[ 0.2969 \sqrt{\frac{x}{c}} - 0.1260 \left(\frac{x}{c}\right) - 0.3516 \left(\frac{x}{c}\right)^2 + 0.2843 \left(\frac{x}{c}\right)^3 - 0.1015 \left(\frac{x}{c}\right)^4 \right] \quad (1)$$

The leading edge of the airfoil approximates a cylinder whose radius can be expressed as

$$r_t = 1.1019ct^2 \quad (2)$$

where  $c$  is the chord length of the airfoil,  $x$  is the position along the chord from the leading edge to the trailing edge, and  $t$  is the maximum thickness as a fraction of the chord [3]. The thickness  $y_t$  does not tend to zero from the above equation at the trailing edge of the airfoil ( $x/c = 1$ ). For computational analysis where zero-thickness may be required, a method can be established with modification of any coefficient to make the sum zero. The last coefficient in Eq. (1) can be revised to -0.1036, which slightly changes the overall airfoil shape. The coordinates ( $x_u, y_u$ ) of the upper airfoil surface, and ( $x_l, y_l$ ) of the lower airfoil surfaces were computed using the equation [2]:

$$x_u = x_l = x ; y_u = +y_t ; y_l = -y_t \quad (3)$$

A NACA 0012 airfoil is selected, designed, and constructed for the present study. The last two digits (00 in the present case) indicate that it is symmetrical; there is no camber at all and 12 indicates that the airfoil is 12% as thick as it is long, which means it has a maximum thickness of 12% to the chord length.

The structured surface profile of the NACA 0012 wing model was developed using SOLIDWORKS software, as shown in Fig. 1.

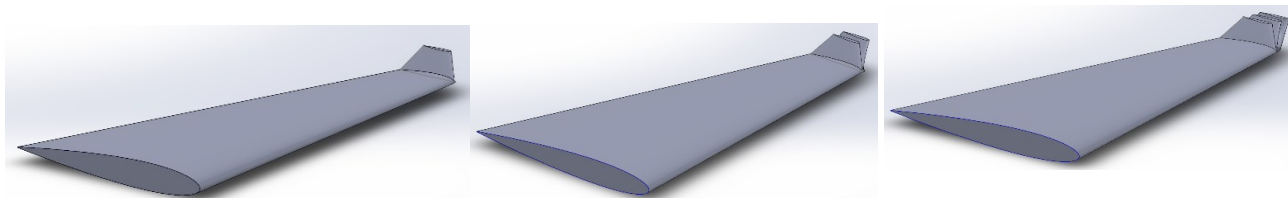


Fig. 1 Wing model of an airplane with one winglet (left), two winglets (middle) and three winglets (right) developed in SOLIDWORKS

To maintain the perfect aspect ratio of chord length to the span of wing, the designed model was printed. It also provides a way to visualize the wing model before the actual construction of it. The wing model was constructed with no geometric and aerodynamic twists to keep things simple so that their effect may be neglected, as shown in Fig. 2. The material used to construct the wing is “Sirish Wood”, whose scientific name is “*Albizia saman*”.

The whole section was made in the woodshop and machine shop of KUET, Khulna. Some wood pieces of required cross sections were taken in the woodshop. Each airfoil section was made very carefully with a soft hand to maintain good accuracy. The wingspan was limited to 30 cm without any sweep. The maximum chord length was 20 cm at the root side, while the minimum was 6 cm at the wing's tip side, making a taper ratio of 0.3. The determination of the average chord length of the wing model was necessary to have the Reynolds number of the same order. Because the exploration of wingtip vortices formation had been a major concern, the Reynolds number based on the average chord length is relevant at low flight speeds. In this sense, the Reynolds number was estimated to be about  $10^5$  in this work. The aspect ratio of the wing signifying the span length relative to the chord length is one of the critical design parameters for the finite wing. The relative weight of the model could be reduced by making it as large as possible.



Fig. 2 Constructed wooden aircraft wing model with three winglets for the experiment in the wind tunnel

The airfoil was drilled with the help of a 1.5 mm diameter drill bit from the wing tip after 1 cm apart from the leading edge to the trailing edge. At the mid-section, a reference point was marked as the center of the winglet. Then the pressure tapping points were drilled at a distance of 2 cm on both sides from the marked reference center. The pressure tapping points on the measuring surfaces were numbered sequentially to track the serial. Then the venial pipes were attached to each of the pressure tapping points. The winglets were not fixed to the wing at the very beginning. At first, one winglet was attached to the wing. It was necessary because an actual size and shape should be checked for one winglet rather than three. The concept was to find the error of construction, if any. The tips of the winglets were made as sharp as possible because there was no curve or round tip was necessary for the present study.

After constructing the wing, the winglets were constructed using the same material and process. The winglets are basically a wing having airfoil shape cross-section that extend from the tip of the wing. However, instead of laying on the same plane of wing, the winglets are non-coplanar structure attached at a certain angle with the plane of the wing at the tip. At first, a single winglet is attached with the main wing body. Subsequently the second and third winglets are attached to the first winglet as presented in Fig. 2. Now the wing with the winglets is ready for testing and to measure the pressures in the wind tunnel. After recording the data, two winglets are attached to the existing one and repeat the procedure to compare the aerodynamic characteristics with the previous one. Afterwards another winglet is attached to the existing two, and so on. The winglets are attached to the wing at the tip.

### 3 Experimental Setup and Procedure

The experimental tests of the study were conducted in the Aerodynamics and Aerial Robotics Laboratory of the Mechanical Engineering Department at Khulna University of Engineering & Technology, Khulna. The laboratory has locally designed and constructed wind tunnel which consists of a subsonic wind tunnel of 1 m × 1 m rectangular test section [26]. The wind tunnel's operational speed limit of airflow can be up to 42 m/s. The turntable of the wind tunnel where the wing models were fitted could set an angle of attack up to 45°. To address the concern of violating the Reynolds number analogy requirements, the aerodynamic characteristics of a large wing model are inspected. A large wind tunnel facility is necessary; therefore, the wing model must be appropriately scaled down to match the usual wind tunnel size. Moreover, there are some limitations in wind tunnel experiments that should be considered; it would be difficult to support the wing model at a desirable height. The size of the wing models was selected so that they could be fitted in the test section of the wind tunnel for the full range of angles of attack.

At the time of constructing the actual model of the section of the wing, an observation was first made about its length compared to the vacant space of the test section. The design created in the software is almost similar when constructing the model in real. The tapping points for pressure tubes were measured. The points were not drilled from the edge of the winglet; a 2 cm gap was maintained. The reason is that the peak value of the lift and drag coefficient will be found at a distance from the trailing edge.

Since the lifting force is necessary to sustain the load of the wing model, placing the constructed model in the test section of the wind tunnel at the beginning of the experiment is crucial. The respective wing models were mounted on the turntable of the wind tunnel test section with the help of a frame. The pressure measuring sensors were the primary instruments for acquiring the test data. The pressure measuring sensors were inserted at

different pre-drilled points from leading to trailing edges, as shown in Fig. 3. Before conducting experiments, precautions were taken, e.g., checking and fixing the specimen model twice before switching ON the wind tunnel and closing the wind tunnel's opening section.



Fig. 3 The wing model placed in the test section of the wind tunnel [26] and pressure tubes are inserted to measure the static pressures

The Bernoulli's principle explains how the energy is conserved between two points of a fluid flow if there is no forced change. This principle was used to determine air velocity in the throat section of the wind tunnel. The airfoil design is symmetrical, so the pressure distribution was desired to be symmetrical on the upper and lower surfaces at zero wing incidences. Using pressure tubes, the pressures on the upper and lower surfaces were measured to ascertain the zero incidences of the wing. The pressures were actively responsive to the change in the angle of attack. To replicate this theoretical change into a practical one for every angle of attack of the airfoil, the pressures were measured. For  $0^\circ$ ,  $5^\circ$ ,  $10^\circ$ ,  $15^\circ$  angles of attack, the respective pressures were determined in the condition of room temperature. There was a limitation of attaching the number of pressure tubes simultaneously, so five pressure tapping points were initially attached to the pressure measuring sensor to the upper surface. After that, with the help of Lab View software, the values of the surface pressures of the airfoil were determined.

The constructed wing of the NACA 0012 section with only one winglet was mounted inside the wind tunnel's test section frame. The testing section began at the first step after setting the angle of attack  $0^\circ$  measurement. The experiment was carried out for different velocities; the pressures were measured simultaneously. Then, the angle of attack was changed to  $5^\circ$ . To examine the changes and compare the differences, the lift and drag forces were measured along with pressure from the relative scales for different velocities. Next, the angles of attack were changed to measure the necessary data in the same way stated before.

A regulator was attached to the wind tunnel by which the velocity of the wind tunnel was controlled. The performed value was taken into 300 volts of the wind tunnel in relation to the room temperature. Barometer recordings showed the ambient pressure, whereas humidity and temperature were determined by a hygrometer and thermometer, respectively, to evaluate air density in the laboratory environment. The tests were carried out with a free-stream velocity of 29.24 m/sec, 34.29 m/sec, and 39.15 m/sec for the respective Reynolds number. For the angle mentioned above of attacks with the help of a pressure sensor, the wing's upper and lower surface pressures were measured. Multiple winglets, i.e., two and then three winglets, were used, and those were triangular. The triangular winglets were attached to the wing at the wingtip. To tackle the issues of experimental

uncertainty and repeatability of test data, considerable attention and precautions are taken during the wind tunnel testing so that confidence can be placed on the results. All the testing were conducted in controlled environment so that the airflow, temperature, and pressure variations are limited in the test section [27].

After measuring the necessary data needed, the calculation process was started. The pressure coefficients on the upper and lower surfaces were calculated from the measured pressure, and the lift coefficient and drag coefficient were calculated using the mathematical relationship of the coefficient of pressure:

$$C_p = \frac{p - p_\infty}{q_\infty} = \frac{p - p_\infty}{\frac{1}{2} \rho_\infty V_\infty^2} \quad (4)$$

where  $p$  is the local static pressure,  $p_\infty$  is freestream pressure,  $V_\infty$  is the free stream velocity, and  $\rho_\infty$  is the free stream density corresponding to the freestream pressure.

From the equation, the value of the  $C_p$  is found, and lift and drag coefficients are calculated by integrating the pressure coefficient over the wing. That is, the coefficient of lift

$$C_L = \frac{1}{c} \int_0^c (C_{p,l} - C_{p,u}) dx \quad (5)$$

and coefficient of drag

$$C_D = \frac{1}{c} \int_0^c \left( C_{p,u} \frac{dy_u}{dx} - C_{p,l} \frac{dy_l}{dx} \right) dx \quad (6)$$

where  $c$  is the chord length,  $C_{p,l}$  is the pressure coefficient at the lower surface and  $C_{p,u}$  is the pressure coefficient at the upper surface [3].

#### 4 Results and Discussion

All the necessary measurements of wind tunnel deploying the constructed aircraft wings with a gradual increase of winglets were conducted. The lift and drag coefficients have been calculated from the experimental pressure coefficient data using Eqs. (4) to (6). Different plots of performance parameters have been drawn to examine the measured data and the calculated results. The coefficients of lift and drag depend on airstream velocity, platform area, profile shape of the airfoil, angle of attack, and angle of winglet (considering the initial position perpendicular with wing). The first two factors determine the dynamic pressure of the airstream. The last three factors mentioned above influence how much drag will be developed in relation to the angle of attack. Therefore, all these factors greatly instigate the coefficient of lift and drag coefficients.

To assess the conditions and conclude the results, systematic analyses are made with the idea of comparing the pressure coefficients against the percentage of chord length for the gradual increase of winglets. It means at first one winglet was considered; next two winglets and three winglets were considered. Three Reynolds numbers were taken randomly, which were calculated based on the free stream velocity at the wind test section. The percentage of chord length was taken up to 100; the interval between them was 10 and started from 0. In the experimental setup, the angles of attack were fixed at  $0^\circ$ ,  $5^\circ$ ,  $10^\circ$ ,  $15^\circ$ . The characteristics of pressure coefficients of the aircraft wing model under test at  $0^\circ$  angle of attack for different Reynolds number are shown in Fig. 4.

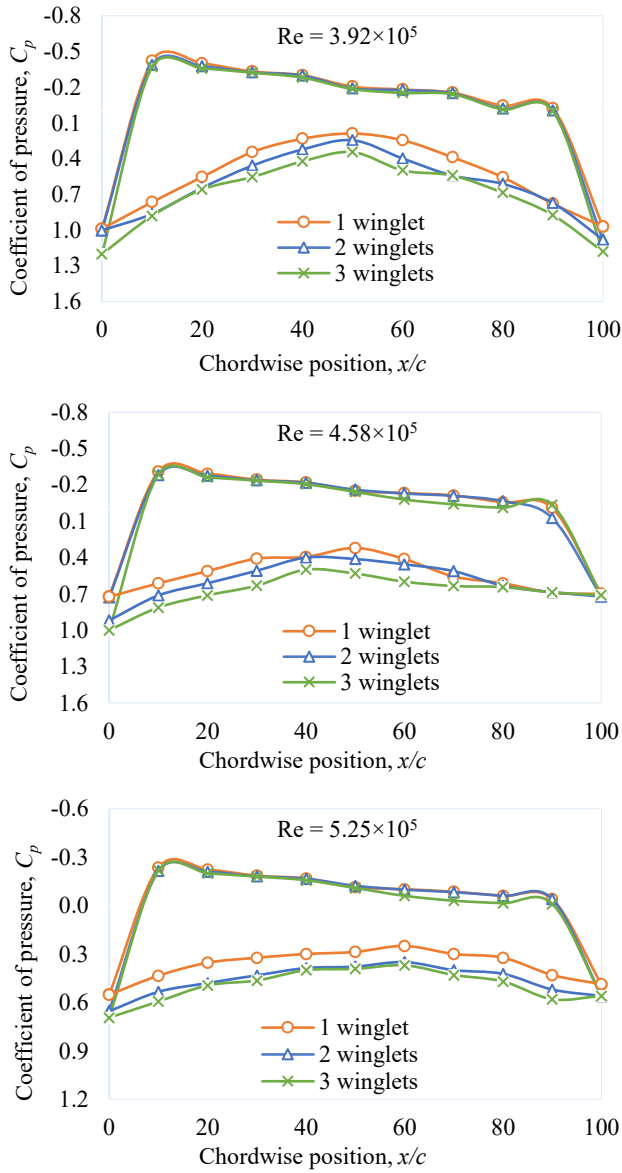


Fig. 4 Distribution of pressure coefficients against the percentage of chord length for different number of winglets and different Reynolds numbers at 0° angle of attack

The plots showed that for the subsequent downstream positions along the chord of the wing, the pressure coefficient reached a certain maximum point (absolute value) for all the three winglet configurations. Just downstream of the leading edge nearly at  $x/c = 20$ , the peak point was observed for the upper surfaces of winglets and then gradually it began to go downward. For the lower surfaces, the peak points are achieved nearly at 50 percent of the chord length. Similar characteristics were monitored for other Reynolds number shown in Fig. 4. The graphs demonstrated that the  $C_p$  at the leading and trailing edges are the same for both the upper and lower surfaces because these points are essentially the same location at 0° angle of attack where the wing model perfectly placed horizontal. It can also be noticed that the two stagnations points at the leading and trailing edges showed the highest  $C_p$  at these positions for all the Reynolds numbers.

The comparison of pressure coefficients at the percentage of chord length positions for the periodic increment of winglets has been illustrated in Fig. 5 for different Reynolds number at 5° angles of attack.

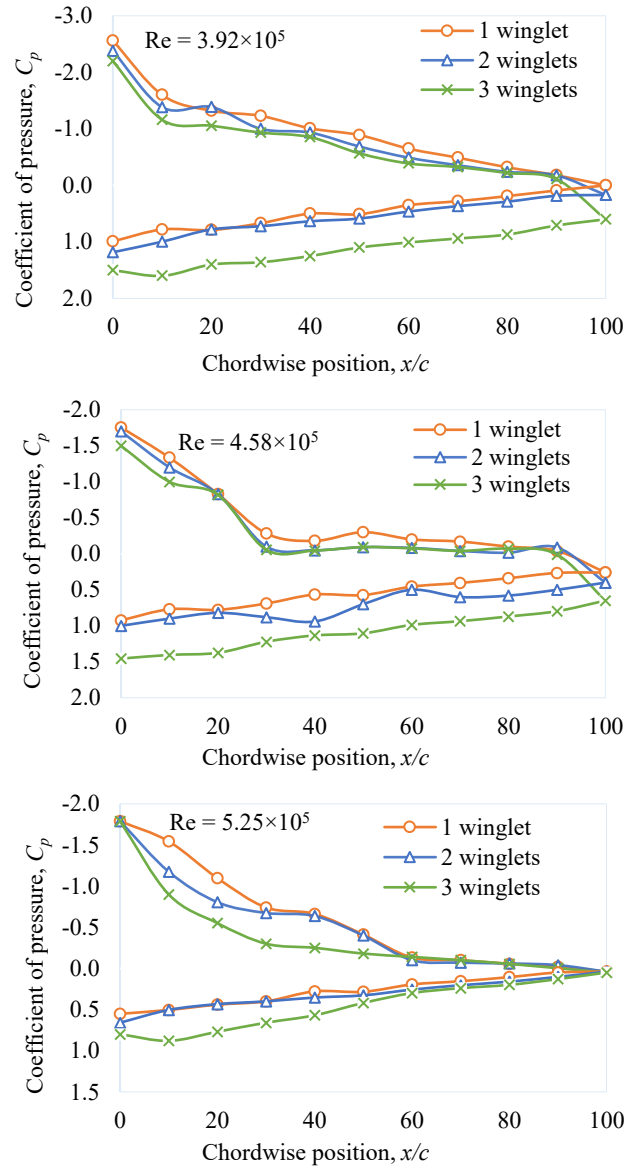


Fig. 5 Variation of pressure coefficients over wing surfaces versus the percentage of chord length for the gradual increase of winglets at 5° angle of attack for various Reynolds numbers

Though the line curves for upper and lower pressure coefficients contrast in their moving in different directions, the major indication is that for a 5° angle of attack, the curve for three winglets is the least one on both occasions. In contrast, the higher values for one winglet gives the elevated  $C_p$  curves for both upper and lower surfaces. Comparing to the  $C_p$  curves at the 0° angle of attack, the value pressure coefficients increased significantly because of higher angle of attack for all three cases of Reynolds number. The pressure coefficient at the upper and lower surfaces near the leading edge are now different value at 5° angle of attack because it is tilted up from the initial horizontal positions at 0°. However, the values at the trailing edge remain the same since trailing edge is very sharp compared to the rounded leading edge of NACA 0012 airfoil.

To identify the variation of the  $C_p$  curves at higher angle of attack, the experiment was carried out with a 10° angle of attack as presented in Fig. 6 for the three Reynolds numbers investigated. The curves have shown look alike characteristics compared to the curves at 5° angle of attack.

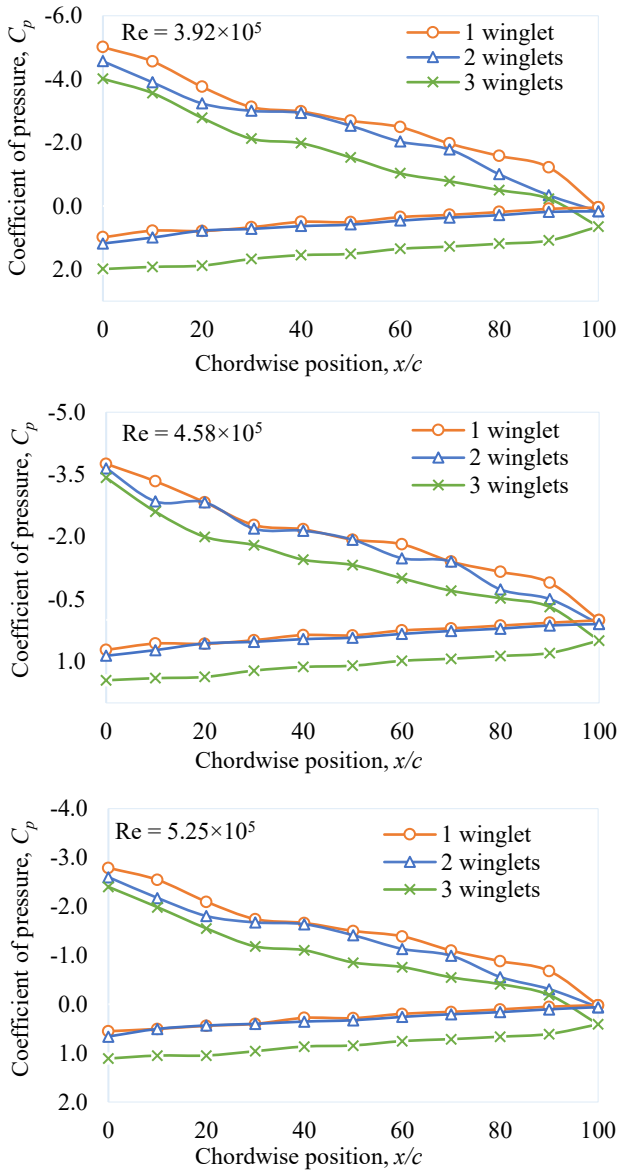


Fig. 6 Comparison of pressure coefficients vs percentage of chord length for the gradual increase of winglets ( $Re = 3.92 \times 10^5$  and  $10^\circ$  angle of attack)

However, the  $C_p$  values at the upper surfaces increased much compared to the respective values at  $5^\circ$  incidence positions for all  $Re$  cases. The values at the lower surfaces not changed greatly indicating the similar pressure distribution between the two angle of attack positions. The curves for the lower surface of the wing are nearly intersected at every point for single and double winglets.

However, for the three winglets, there is a clear distinction with the other two curves for both the upper and lower sides of the winglets.

Again, the pressure coefficients in Fig. 7 suggested that for the  $15^\circ$  angle of attack and the different Reynolds numbers, the coefficients give an elevated curve for one winglet. In contrast, the bottom one has been a standstill for the case of three. The middle curve is the wing containing three winglets for both the upper and lower positions. Observing the  $C_p$  curves in Fig. 4 to Fig. 7 for all the angle of attack ranging  $0$ - $15^\circ$  demonstrated that increasing the Reynolds number decreases the pressure coefficients specially at the upper surface.

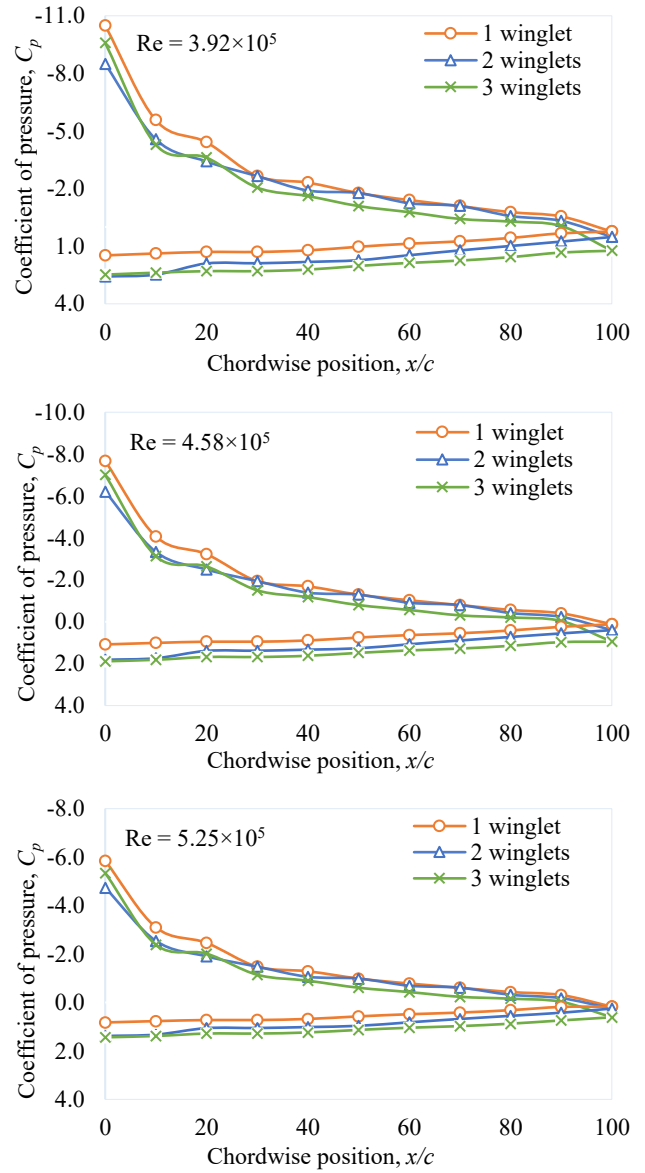


Fig. 7 Pressure distribution comparison on the upper and lower surfaces in different chord positions of wing model for the single and multi-winglets configuration at  $15^\circ$  angle of attack for various Reynolds number

Keeping in mind that the lift generated in a wing is the net difference between the upper and lower surface pressure; the above trend suggest that higher flight velocities generate less lift coefficient.

The characteristics of pressure coefficients of the wing model at  $5^\circ$ ,  $10^\circ$ , and  $15^\circ$  angles of attack are shown in Fig. 5, Fig. 6, and Fig. 7, respectively. The curves showed very similar characteristics for both upper and lower surfaces. However, the pressure coefficient of the upper surfaces begins from a certain maximum point for all three winglets and then gradually goes downward. Therefore, with the increase of the angle of attack, the peak point of the pressure coefficient on the upper surface is shifting towards the leading edge. On the other hand, the peak points are achieved nearly at 100 percent of chord length for the lower surfaces. Gradual increase of pressure coefficient for the lower surface had been increasing with the percentage of chord length. After consulting the characteristics of pressure coefficient plots of Fig. 5, Fig. 6, and Fig. 7, suggests that for  $0^\circ$ ,  $5^\circ$ ,  $10^\circ$ ,  $15^\circ$  angle of attack and all the considered Reynolds

numbers, the coefficient of lift may be calculated to have a higher value when the wing consists of three winglets rather than one or two. The above results could conclude that using three winglets in a wing is more effective because the pressure difference is more than the other two for all three Reynolds numbers.

After analyzing the pressure distributions through the pressure coefficient plots, the average pressure coefficients are calculated for different angles of attack at Re value of  $5.25 \times 10^5$ , and plotting them in a graph as displayed in Fig. 8.

After analyzing the curves, it can be said that a stable and similar nature was shown for a range angle of attack starting from  $0^\circ$  up to  $15^\circ$ . The average pressure coefficient is decreasing in upper surface and that of the lower surface is increasing making the difference between the two surfaces diverging for all the winglet configurations. This suggest that lift increases at higher angle of attack positions. However, some deviation could be seen for the three different numbers of winglet arrangements. For three winglets arrangement, the curves are lowest for both the upper and lower surfaces of the wing. A decisive statement could be drawn from this those changes in the curves that the increment of the angle of attack increases the net change of average pressure coefficients, consequently increasing the lift coefficient.

Another approach was taken to compare the effects of Reynold’s number on average pressure coefficients. The average pressure coefficient for the upper and lower surfaces at  $5^\circ$  angle of attack are plotted against the Reynolds numbers in Fig. 9. The figure illustrates a contrasting pattern for the upper and lower curves for all three different configurations of winglets. However, the curve for three winglets is the bottom one for the lower surface, while for the upper surface, the higher curve is for three winglets. Hence, with the increase of Reynold’s number, the average pressure coefficient for the upper surface is decreases, whereas the gradual increment could be seen for the lower one with the increment of Reynold’s number. The plots clearly demonstrating that increasing the Re decreases the net difference between of average  $C_p$ , reduces the lift at higher values of Re.

The main objective was to calculate the lift and drag coefficients from the pressure coefficients. The lift coefficient can be said as “the ratio between the lift force and the product of dynamic pressure and area”. It is one of the measures of the effectiveness of airfoil to produce lift.

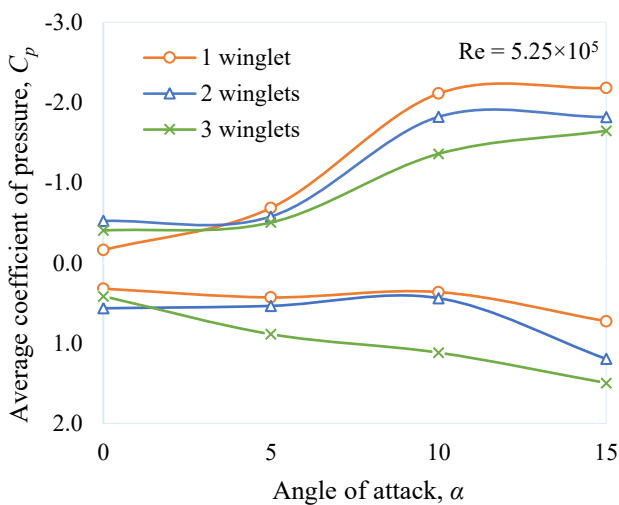


Fig. 8 Average pressure coefficients vs angle of attack for the gradual increase of winglets

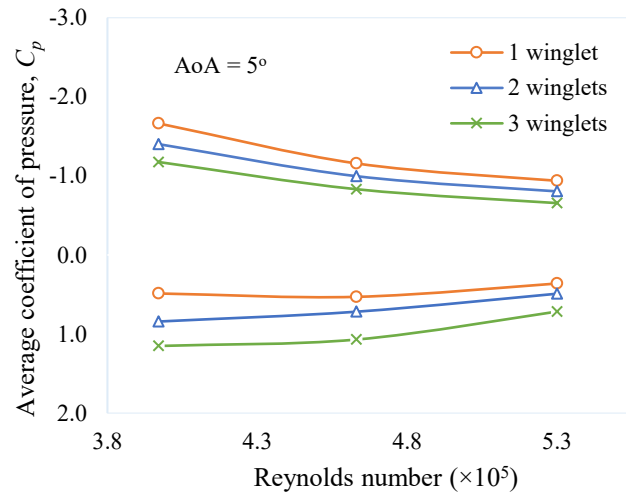


Fig. 9 Average pressure coefficients vs Reynolds number for the gradual increase of winglets

The values of lift coefficients varying with different angles of attack have been obtained from experimental data. The importance of the angle of attack in determining wing performance cannot be overemphasized. The lift characteristic is also dependent upon or affected by thickness distribution and location of maximum thickness, camber, and other factors such as increasing the thickness, which results in lower static pressure and more lift.

The lift coefficient variation with angle of attack at  $5.25 \times 10^5$  Reynolds number was represented in Fig. 10. Observing the curves for one, two, and three winglets indicate a better lift coefficient when three winglets were attached with the main wing body for different angles of attack. The maximum lift coefficient of 1.97 was obtained near  $10^\circ$  angle of attack for three winglets arrangement. After that, all three curves are declining indication stalling of the wing that occurred because of the flow separation on the upper surface of wing. In Fig. 11, the drag coefficient for the incremental angle of attack for the arrangements at  $5.25 \times 10^5$  Reynolds number is presented. The curves clearly showing that increasing the angle of attack increasing the drag coefficients for all the cases because of higher pressure drag on the wing models. The pressure drag on the wing increases with the increase of angle of attack due to its shift from the streamlined position at  $0^\circ$  incidence with respect to freestream direction.

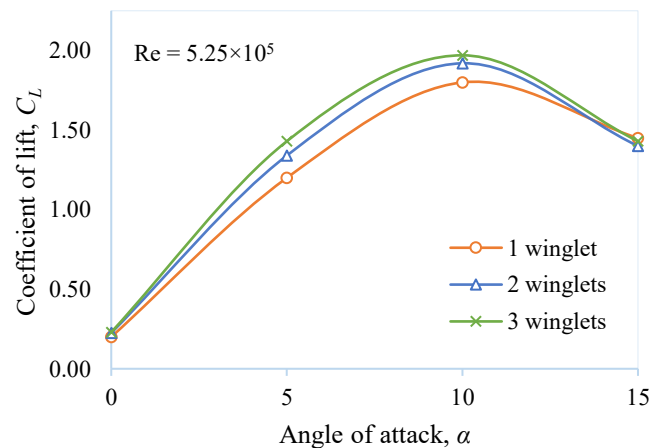


Fig. 10 Variation of lift coefficient with angle of attack for the multi-winglet configurations at  $Re = 5.25 \times 10^5$

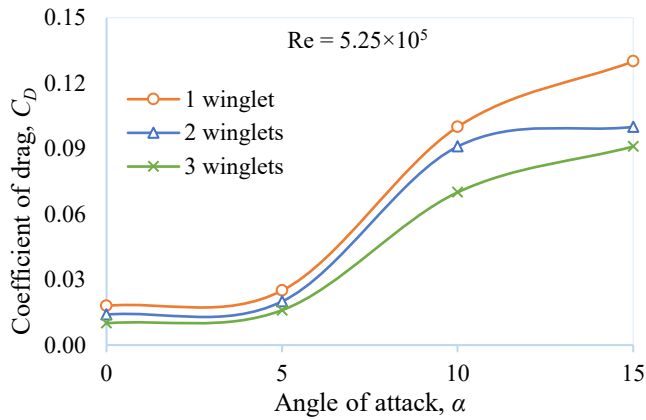


Fig. 11 Variation of drag coefficient with angle of attack for the multi-winglet configurations at  $Re = 5.25 \times 10^5$

The  $C_D$  values for one winglet are higher than the other two conditions. Moreover, the drag coefficients are lower for three winglets arrangement. It is a diligent way of reflecting on the advantages of three winglets. However, skin friction drag may occur, but induced drag is the primary factor contributing more to drag formation in winglets. This is why adding more winglets after using three, could have obtained lower values.

Lift-to-drag ratio is another significant tool to evaluate the performance of a wing with single or multi-winglets. Computational research work showed that multi-winglets could yield significant reductions of induced drag in the lower two-digit percentage range compared to planar wing concepts having the same wing area and span [28]. The lift-to-drag ratio for different angles of attack is presented in Fig. 12 at  $Re = 5.25 \times 10^5$ . From the figure, it is seen that the ratio of lift to drag is higher at the beginning of the angle of attack for two winglets, but as the angle of attack, the value of lift to drag ratio rises for three winglets. However, a peak value has been obtained around  $5^\circ$  angle of attack. This behavior is because when the angle of attack is increased until the lift-to-drag ratio reaches its maximum value, both  $C_L$  and  $C_D$  increase, but  $C_L$  increases more than  $C_D$ . The maximum lift-to-drag ratios for one-, two-, and three-winglets configurations are found to 48, 67, 89, respectively, at  $5^\circ$  angle of attack for all cases. As the lift-to-drag ratio is considered as the aerodynamics efficiency of an aircraft, this value of  $5^\circ$  AoA can be taken as the cruise angle of attack in the multi-winglet configuration. This finding of the study is consistent with the findings of literature [2].

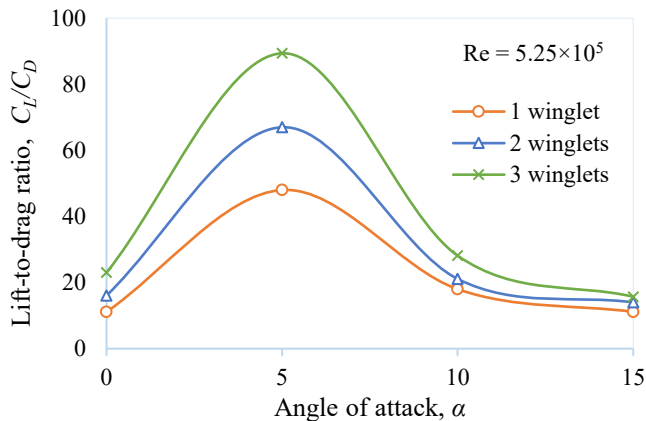


Fig. 12 Variation of lift-to-drag ratio with the angle of attack for the multi-winglet configurations at  $Re = 5.25 \times 10^5$

## 5 Conclusions

It has long been theoretically stamped that winglet can be a phenomenal addition in the wing to reduce the induced drag. However, the actual performance of technical adaptations of multi-winglet configurations often fell short of the expectations raised by the theoretical predictions. The experimental data from this work confirmed the improvements in aerodynamic coefficients by using multi-winglets. The pressure distribution on the surfaces of the wing varies to the angle of attack and Reynolds number considerably. The maximum lift producing point (minimum pressure point) on the upper surface moves towards the leading edge from the percentage of chord position of 20% at  $0^\circ$  with the increase of angle of attack. It is depicted from the drag and lift coefficient graphs that the use of multiple winglets increases the lift coefficient and reduces the drag coefficient. The experimental results also showed that the wing with a gradual increase of winglets can reduce the induced drag and improve the value considerably compared with the wing without winglets. For all cases, a wing with one winglet showed less advantages than the two or three-winglet configurations. In particular, the pressure coefficients for lower and upper surfaces indicated that a wing with three winglets provides a better lift coefficient and reduces drag coefficient. Accordingly, three winglets provide more benefits as the results suggested. From all the points of view, multiple winglets are advantageous over single or no winglets in the wing. It is expected that shape of the winglet and appropriate selection of the geometrical parameters of the winglet may further improve the aerodynamic performance of the wing which can be investigated both numerically and experimentally in the future.

## Nomenclature

$c$	Chord length (m)
$C_D$	Coefficient of drag (-)
$C_L$	Coefficient of lift (-)
$c_p$	Coefficient of pressure (-)
$p$	Actual pressure of the body ( $N/m^2$ )
$p_\infty$	Free stream pressure ( $N/m^2$ )
$S$	Wing surface area ( $m^2$ )
$t$	Maximum thickness (m)
$V_\infty$	Free stream velocity (m/sec)
$\alpha$	Angle of attack (degree)
$\mu_\infty$	Free stream viscosity (kg/m.sec)
$\rho_\infty$	Free stream density ( $kg/m^3$ )
AoA	Angle of attack (degree)
Re	Reynolds number (-)

## Acknowledgments

The authors warmly recognize the wind tunnel testing facilities at the Department of Mechanical Engineering, KUET, Bangladesh. The authors are indebted to Md. Mushfiqur Rahman of KUET for helping in the CAD modeling of the wing model.

## Conflict of Interest

There is no known conflict of interest associated with this publication and there has been no significant financial support for this work that could have influenced its outcome.

## References

- [1] Khan, M.M.I. and Al-Faruk, A., 2018. Comparative analysis of aerodynamic characteristics of rectangular and curved leading edge wing planforms. *American Journal*

- of *Engineering Research (AJER)*, 7(5), pp.281-291. Available at: <www.ajer.org>.
- [2] Anderson, J.D. Jr., 2011. *Fundamentals of aerodynamics*. 5th ed. New York: McGraw-Hill.
- [3] Houghton, E.L., Carpenter, P.W., Collicott, S.H. and Valentine, D.T., 2017. *Aerodynamics for engineering students*. 7th ed. Oxford: Butterworth-Heinemann.
- [4] Coimbra, R.F.F. and Catalano, F.M., 1999. Estudo experimental sobre pontas de asa para uma aeronave agrícola. *Revista Brasileira de Engenharia Agrícola e Ambiental*, 3(1), pp.99-105.
- [5] Krishnan, S.G., Ishak, M.H., Nasirudin, M.A. and Ismail, F., 2020. Investigation of aerodynamic characteristics of a wing model with RGV winglet. *Journal of Aerospace Technology and Management*, 12, e2020.
- [6] Smith, M., Komerath, N., Ames, R., Wong, O. and Pearson, J., 2001. Performance analysis of a wing with multiple winglets. *19th AIAA Applied Aerodynamics Conference*. Reston, Virginia: American Institute of Aeronautics and Astronautics. doi:10.2514/6.2001-2407.
- [7] Kroo, I., McMasters, J. and Smith, S.C., 1996. Highly nonplanar lifting systems. *Transportation Beyond 2000: Technologies Needed for Engineering Design*.
- [8] Yates, J.E. and Donaldson, C.D., 1986. A fundamental study of drag and an assessment of conventional drag-due-to-lift reduction devices, *NASA Technical Report*, NASA-CR-180891.
- [9] Ismail, N., Usman, K.M., Balogun, M.B., Abdullahi, M., Faru, F.T. and Ibrahim, I., 2020. Effect of angle of attack on lift, drag, pitching moment and pressure distribution of NACA 4415 wing. *Journal of Science Technology and Education*, 8(1), pp.31-44.
- [10] Al-Atabi, M., 2006. Aerodynamics of wing tip sails. *Journal of Engineering Science and Technology*, 1(1), pp.89-98.
- [11] Eftekhari, S. and Al-Obaidi, A.S.M., 2019. Investigation of a NACA0012 finite wing aerodynamics at low Reynold's numbers and 0o to 90o angle of attack. *Journal of Aerospace Technology and Management*, 11, e1519.
- [12] Cerón-Muñoz, H.D. and Catalano, F.M., 2006. Experimental analysis of the aerodynamic characteristics adaptive of multi-winglets. *Proceedings of the Institution of Mechanical Engineers, Part G: Journal of Aerospace Engineering*, 220(3), pp.209-215.
- [13] Inam, M.I., Mashud, M., Al-Nahian, A. and Selim, S.M.S., 2010. Induced drag reduction for modern aircraft without increasing the span of the wing by using winglet. *International Journal of Mechanical & Mechatronics Engineering IJMME-IJENS*, 10(3), pp.49-53.
- [14] Sayem, M.S.H., Sagar, M.M., Alam, R. and Al-Faruk, A., 2024. Numerical analysis of aerodynamic characteristics of aeroplane wing with winglets. *International Research Journal of Engineering and Technology*, 11(5), pp.1601-1622.
- [15] Sayem, M.S.H. and Al-Faruk, A., 2020. Effect of cant angles on the aerodynamic performances of an airplane wing with blended type winglet: Numerical analysis. *International Conference on Mechanical, Industrial and Energy Engineering*. Khulna.
- [16] Yusoff, H. et al., 2022. The evolution of induced drag of multi-winglets for aerodynamic performance of NACA23015. *Journal of Advanced Research in Fluid Mechanics and Thermal Sciences*, 93(2), pp.100-110. doi:10.37934/arfmts.93.2.100110.
- [17] Reddy, S.R., Sobieczky, H., Dulikravic, G.S. and Abdoli, A., 2016. Multi-element winglets: Multi-objective optimization of aerodynamic shapes. *Journal of Aircraft*, 53(4), pp.992-1000. doi:10.2514/1.C033334.
- [18] Padmanathan, P. et al., 2024. Parametric optimization study of novel winglets for transonic aircraft wings. *Applied Sciences*, 14(17), p.7483. doi:10.3390/app14177483.
- [19] Sethunathan, P., Ramasamy, K.K., Sivasubramaniam, A.P. and Kannan, R., 2024. Aerodynamic performance of semi-wing with multiple winglets operating at low- and medium-range Reynolds numbers. *International Journal of Modern Physics C*, 35(10), p. 2450134.
- [20] Bala, M.N.V.S.S., Kalali, S.K.G., Goud, B.N., Kumar, A.S. and Gupta, M.S., 2023. Flow investigation of a multiple winglet wing model. *AIP Conference Proceedings*, 2492 (1), p.020002.
- [21] El Haddad, N., 2015. Aerodynamic and structural design of a winglet for enhanced performance of a business jet. *Master's Thesis, Embry-Riddle Aeronautical University*.
- [22] Lovegren, J. and Hansman, R.J., 2011. Estimation of potential aircraft fuel burn reduction in cruise via speed and altitude optimization strategies, *Master's Thesis, Massachusetts Institute of Technology*.
- [23] Ulrich, L., Roche, L. and Consulting, L.R., 2001. Induced drag reduction with the WINGGRID device. *Aerodynamic Drag Reduction Technologies*. Berlin, Heidelberg: Springer Berlin Heidelberg, pp.304-311. doi:10.1007/978-3-540-45359-8\_32.
- [24] Ebrahimi, A. and Mardani, R., 2018. Tip-vortex noise reduction of a wind turbine using a winglet. *Journal of Energy Engineering*, 144(1), p. 04017052.
- [25] Yin, K., 2017. A study of carbon dioxide emissions reduction opportunities for airlines on Australian international routes. *Master's Thesis, The University of Queensland, Brisbane*.
- [26] Arifuzzaman, M. and Mashud, M., 2012. Design construction and performance test of a low-cost subsonic wind tunnel. *IOSR Journal of Engineering (IOSRJEN)*, 2(10), pp.83-92.
- [27] Rahman, M.M., Shayor, A.A., Al-Faruk, A. and Evan, M.T.R., 2025. Numerical investigation with experimental validation of aerodynamics performance of NACA 2414 airfoil with passive momentum injection through channeling. *Results in Engineering*, 25, p.104533.
- [28] Berens, M., 2008. Potential of multi-winglet systems to improve aircraft performance, *Master's Thesis, Technical University Berlin, Berlin*.